RESEARCH ARTICLE

Plasma metabolomics of presymptomatic *PSEN1*-H163Y mutation carriers: a pilot study

Karthick Natarajan[1,2,a] , Abbe Ullgren[1,2,a], Behzad Khoshnood[1,2], Charlotte Johansson[1,2], José M. Laffita-Mesa[1,2], Josef Pannee[3], Henrik Zetterberg[4,5], Kaj Blennow[3] & Caroline Graff[1,2]

[1]Division for Neurogeriatrics, Centre for Alzheimer Research, Department of Neurobiology, Care Sciences and Society, Karolinska Institutet, Stockholm, Sweden
[2]Unit for Hereditary Dementias, Theme Aging, QA12, Karolinska University Hospital-Solna, Stockholm, Sweden
[3]Institute of Neuroscience and Physiology, Department of Psychiatry and Neurochemistry, The Sahlgrenska Academy at the University of Gothenburg, Gothenburg, Sweden
[4]Institute of Neuroscience and Physiology, Department of Psychiatry and Neurochemistry, The Sahlgrenska Academy at the University of Gothenburg, Gothenburg, Sweden
[5]Department of Molecular Neuroscience, UCL Institute of Neurology, London, WC1N 3BG, England

Correspondence
Karthick Natarajan and Caroline Graff, Department NVS, Division of Neurogeriatrics, Karolinska Institutet, Bioclinicum J10:20, Visionsgatan 4, 171 64, Solna, Sweden. Tel: +46 723 821 813 (K.N.); Tel: +46(0)73 383 9399 (C.G.); E-mails: karthickn1982@gmail.com; caroline.graff@ki.se

[a]Shared first authors.

Abstract

Background and Objective: *PSEN1*-H163Y carriers, at the presymptomatic stage, have reduced [18]FDG-PET binding in the cerebrum of the brain (Scholl et al., Neurobiol Aging 32:1388–1399, 2011). This could imply dysfunctional energy metabolism in the brain. In this study, plasma of presymptomatic *PSEN1* mutation carriers was analyzed to understand associated metabolic changes. **Methods**: We analyzed plasma from noncarriers (NC, $n = 8$) and presymptomatic *PSEN1*-H163Y mutation carriers (MC, $n = 6$) via untargeted metabolomics using gas and liquid chromatography coupled with mass spectrometry, which identified 1199 metabolites. All the metabolites were compared between MC and NC using univariate analysis, as well as correlated with the ratio of $A\beta_{1-42}/A\beta_{1-40}$, using Spearman's correlation. Altered metabolites were subjected to Ingenuity Pathway Analysis (IPA). **Results**: Based on principal component analysis the plasma metabolite profiles were divided into dataset A and dataset B. In dataset A, when comparing between presymptomatic MC and NC, the levels of 79 different metabolites were altered. Out of 79, only 14 were annotated metabolites. In dataset B, 37 metabolites were significantly altered between presymptomatic MC and NC and nine metabolites were annotated. In both datasets, annotated metabolites represent amino acids, fatty acyls, bile acids, hexoses, purine nucleosides, carboxylic acids, and glycerophosphatidylcholine species. 1-docosapentaenoyl-GPC was positively correlated, uric acid and glucose were negatively correlated with the ratio of plasma $A\beta_{1-42}/A\beta_{1-40}$ ($P < 0.05$). **Interpretation**: This study finds dysregulated metabolite classes, which are changed before the disease symptom onset. Also, it provides an opportunity to compare with sporadic Alzheimer's Disease. Observed findings in this study need to be validated in a larger and independent Familial Alzheimer's Disease (FAD) cohort.

Introduction

Alzheimer's disease (AD) is a growing health concern estimated to affect 136 million people worldwide by 2050.[1] The autosomal dominant mutations found in the *APP*, *PSEN1*, and *PSEN2*[2] genes cause early-onset Familial Alzheimer's Disease (FAD), with the high penetrance *PSEN1* mutations (https://www.alzforum.org/mutations/psen-1) being the most frequent.[3] PSEN1 is a part of the gamma-secretase protein complex, which cleaves the Amyloid precursor protein (APP) that leads to the production of a mixture of amyloid peptides $A\beta_{1-40}$ (90%)

and $A\beta_{1-42}$ (10%) in the amyloidogenic pathway.[3] These peptides are known to be part of the pathobiology of FAD. The *PSEN*1 mutation p.His163Tyr (*PSEN1*-H163Y) results in higher ratios of $A\beta_{1-42}/A\beta_{1-40}$[4] in in vitro assays.

Previously, several studies have described the plasma metabolic profile of sporadic mild cognitive impairment (MCI) and AD cases.[1,5–10] A targeted plasma lipid profiling was performed in *PSEN1* mutation carriers.[11] However, no untargeted plasma metabolome has yet been reported for presymptomatic *PSEN1* mutation carriers.

In FAD, the preclinical phase is characterized by brain glucose hypometabolism.[12,13] We have previously demonstrated glucose hypometabolism in the cerebrum at the presymptomatic stage of *PSEN1*-H163Y carriers.[14] In this follow-up study, we hypothesize that untargeted plasma metabolite profiling could provide clues about the dysregulated metabolic pathways in presymptomatic *PSEN1* mutation carriers (MC) in comparison with noncarriers (NC) within the FAD *PSEN1*-H163Y cohort.[2,15–17] First, we identified metabolites, which are differentially expressed between MC and NC and assessed their associated biological processes. Then, we explored the association between these metabolites with plasma levels of various amyloid beta isoforms ($A\beta$). Taken together, our study provides a snapshot of the plasma metabolic changes in presymptomatic *PSEN1* MC, which may inform about biological events that are characteristics of the preclinical phase.

Materials and Methods

Study population

Relatives with plasma samples from the *PSEN1*-H163Y kindred in the Swedish FAD study were eligible for inclusion. The prospective FAD study invites *APP* and *PSEN1* kindreds at the Memory outpatient clinic in Karolinska University Hospital, Stockholm, since 1993. Presymptomatic relatives with 50% risk of disease are followed longitudinally with a comprehensive assessment battery, described in detail elsewhere.[2,15,17] Clinical and neuroradiological evaluations are accompanied by sampling of cerebrospinal fluid (CSF) and blood. Mean (SD) age of onset in the *PSEN1*-H163Y kindred is 52 ± 6 years (based on 12 individuals). Symptom onset is regarded as having the first subjective symptoms as experienced by participants or next-of-kin. Mutation status (carrier or noncarrier) was not known to participants or clinicians within the study, if not stated otherwise. The study procedures were approved by the Regional Ethical Review Board in Stockholm, Sweden, and were in agreement with the Helsinki Declaration. Study participants provided written informed consent. The plasma samples were collected in a longitudinal manner as a part of the battery of clinical evaluation over the years from 1995 to 2017.

DNA extraction from blood

As part of the FAD study protocol, venous blood was collected at the Memory clinic of Karolinska university hospital, Stockholm. Using the Gentra Puregene blood Kit (Qiagen, Hilden, Germany) DNA was extracted from the blood and resuspended in RNase & DNase free water (Qiagen, Hilden, Germany). The concentration of extracted DNA was measured with the QUBIT instrument (Thermofisher, Waltham, MA, USA) as described by the manufacturer.

Genotyping for *PSEN1*-H163Y mutation

20ng of DNA was amplified for *PSEN1*-Exon6 using forward (5' GGTTGTGGGACCTGTTAATT 3') and reverse (5' CAACAAAGTACATGGCTTTAAATGA 3') primers with AmpliTaq Gold® 360 PCR Master Mix (Thermofisher, Waltham, MA, USA). Sanger sequencing was performed using BigDye™ Terminator v3.1 Cycle Sequencing Kit (Thermofisher, Waltham, MA, USA) in both forward and reverse directions and analyzed using ABI3500 Genetic Analyzer (Thermofisher, Waltham, MA, USA).

APOE allele genotyping

The *APOE* genotyping was performed for SNP rs7412 and rs429358 using predesigned TaqMan® SNP Genotyping Assays (Thermofisher, Waltham, MA, USA) as indicated in the manufacturer's protocol. The amplified products were run on 7500 fast Real-Time PCR Systems (Thermofisher, Waltham, MA, USA).

Plasma sample collection

Nonfasting plasma was prepared from the blood. The plasma was removed as the supernatant after 1 h incubation at room temperature (RT) and 10 min centrifugation at 2200*g*. Then, the plasma was aliquoted and frozen at −80°C until analysis. Plasma sampled between the years 1995 to 2017 were included. The metabolite analysis was carried out at the Swedish Metabolomics Center (SMC, https://www.swedishmetabolomicscentre.se/), Umeå, Sweden.

Metabolite extraction and analysis

Untargeted metabolite extraction and analysis via Gas Chromatography (GC) and Liquid Chromatography (LC)

in combination with Mass-Spectrometry (MS) were performed at SMC as described here.[18] Plasma was prepared by adding 900 μL of extraction buffer (90/10 v/v methanol: water) along with internal standards for the GC–MS and LC–MS to 100 μL of plasma. The samples were prepared and analyzed in a randomized order for GC–MS and LC–MS. Detailed methods were described in the Data S1 section (Metabolite profiling of the plasma).

Analysis of $A\beta_{1-38}$, $A\beta_{1-40}$, and $A\beta_{1-42}$ in plasma

The analyses of $A\beta_{1-38}$, $A\beta_{1-40}$, and $A\beta_{1-42}$ in plasma were performed using immunoprecipitation coupled to tandem Liquid Chromatography mass spectrometry (IP-LC–MS/MS) as described previously.[19,20] In short, calibrators were prepared using recombinant $A\beta1-38$, $A\beta1-40$, and $A\beta1-42$ (rPeptide) added to 8 % bovine serum albumin in phosphate-buffered saline. Recombinant ^{15}N uniformly labeled $A\beta_{1-38}$, $A\beta_{1-40}$, and $A\beta_{1-42}$ (rPeptide) were used as internal standards (IS), added to samples and calibrators prior to sample preparation. $A\beta$ peptides were extracted from 250 μL human plasma using immunoprecipitation with anti-β-Amyloid 17–24 (4G8) and anti-β-Amyloid 1–16 antibodies (6E10, both Biolegend®) coupled to Dynabeads™ M-280 Sheep Anti-Mouse IgG magnetic beads (Thermofisher, Waltham, MA, USA). Immunoprecipitation was performed using a KingFisher™ Flex Purification System (Thermofisher, Waltham, MA, USA). Analysis of processed samples was performed using liquid chromatography-tandem mass spectrometry (LC–MS/MS) on a Dionex Ultimate LC-system and a Thermo Scientific Q Exactive quadrupole-Orbitrap hybrid mass spectrometer. Chromatographic separation was achieved using basic mobile phases and a reversed-phase monolith column at a flow rate of 0.3 mL/min. The mass spectrometer operated in parallel reaction monitoring (PRM) mode was set to isolate the 4+ charge state precursors of the $A\beta$ peptides. Product ions (14–15 depending on peptide) specific for each precursor was selected and summed to calculate the chromatographic areas for each peptide and its corresponding IS. The area ratio of the analyte to the internal standard in unknown samples and calibrators was used for quantification.

Statistical analysis

All statistical analyses were done using R (The R Foundation for Statistical Computing; version 3.6.1) and R Studio software. Group comparisons between presymptomatic *PSEN1*-H163Y MC and NC were made using Wilcoxon rank-sum tests and a *P* value below 0.05 was considered as significant. Features with *P* values above the significance

threshold were excluded from downstream analysis. Correlations between the selected metabolites and plasma $A\beta_{1-42}/A\beta_{1-40}$ ratio were tested using Spearman's rho statistic and the *P* values were calculated using the asymptotic t approximation.

The correlation between the observed metabolite levels and how many years the sample had been kept in storage was tested using Spearman's rho statistic and the *P* values were calculated using the asymptotic t approximation. The same was done for correlations with participant age at sampling and the presence of at least one *APOE*ε4 allele. The heatmaps were constructed using two separate clusters, one cluster for the features and another for the samples. The clustering analysis was done using agglomerative hierarchical clustering using the Wards clustering criterion. The dissimilarity matrices were constructed using Pearson's correlation.

Metabolites biological interpretation

Differential metabolites between MC and NC were converted into their corresponding Human Metabolome Database identifier (http://www.hmdb.ca/, HMDB ID) as well as annotated for their metabolite class. HMDB ID was analyzed using the Ingenuity Pathway Analysis (IPA)[21] (https://www.qiagenbioinformatics.com/products/ingenuity-pathway-analysis/, Qiagen Inc.) software, enriched significant metabolite ontologies were filtered as described in the IPA's metabolomics white paper (http://pages.ingenuity.com/rs/ingenuity/images/wp_ingenuity_metabolomics.pdf).

Results

Demographics of the study population

A total of 24 plasma samples from 17 males were included in this study, of these there were 6 mutation carriers (MC) and 11 noncarriers (NC). The study participants were relatives from the *PSEN1*-H163Y kindred, except for three NC from two *APP* kindreds which were included to increase the number of available controls (Table 1). The participants underwent repeated sampling of blood, meaning these individuals were represented more than once and contributing to an overall mean age at sampling of 42 ± 11 years. Distribution of mutation status, *APOE*ε4 status and mean age at sampling in each dataset are described in Table 1. Asymptomatic status in all participants was confirmed by later records of the actual age of onset in the MC and mean Mini-Mental State Examination (MMSE) scores[22] were 29 ± 1 (maximum score 30) upon sampling. One of the participants from the MC group opted for presymptomatic genetic

Table 1. Demographics of the study participants

| Dataset | A | | B | |
Genetic status	presymptomatic MC	NC	presymptomatic MC	NC
Total number of individuals (samples)	6	8	4	6
PSEN1 kindred	6	5	4	3
APP kindred	0	3	0	3
Age (y) (Mean $\pm$ SD)	35 $\pm$ 5.97	39.63 $\pm$ 8.83	48.5 $\pm$ 5.8	49.67 $\pm$ 16.13
MMSE (Mean $\pm$ SD)	29 $\pm$ 1	–	29 $\pm$ 1	–
APOEε4 carrier %	50%	50%	50%	50%

Demographic data for dataset A (samples collected before 2008) and dataset B (samples collected after 2008), which were used for the univariate analysis. Plasma samples were stratified for univariate analysis based on the PCA (Fig. S1). One "baseline" plasma sample from each time period was selected, and all individuals were male and presymptomatic upon sampling. The number of Apolipoprotein E4 (*APOEε4*) genotype carriers in each dataset is indicated. Seven of the participants (3 NC and 4 MC) are represented in both A and B datasets ("y" denotes years).

testing at the hospital. This has since proved to be a rare case of reduced penetrance, showing no signs of beta-amyloid ($A\beta$) retention during [11C]Pittsburgh compound B (PiB) positron emission tomography (PET) at the age of 60 years[15] and no cognitive deficits during the most recent psychological assessment, performed at the age of 65, 13 years past the expected age of onset. There were no known subjects with alcohol overconsumption or dietary restrictions.

Comparison of plasma metabolite levels between presymptomatic MC and NC

Untargeted GC–MS and LC–MS analysis of the plasma samples detected 1199 metabolites, of which 23% were annotated. First, a Principal Component Analysis (PCA) model was built (Fig. S1). The PCA analysis indicate a clear separation of the samples based on the number of years of storage. A similar effect was previously reported.[23] For that reason, the samples were stratified into two separate datasets based on the sample collection year (Table 1; referred to as dataset A and B in the text). Dataset "A" contains the samples collected before the year 2008 and dataset "B" contains the samples collected after 2008.

The two datasets were analyzed separately. Within them the measured levels of the metabolites were compared between the MC and NC. In dataset A, the levels of 79 metabolites (14 annotated), were significantly different in MC compared with NC ($P < 0.05$) (Table 2, Table S1). The annotated metabolites belong to the metabolite classes of amino acids ($n = 3$), carboxylic acids ($n = 1$), hexoses ($n = 1$), imidazopyrimidines ($n = 1$), fatty acyls ($n = 1$), glycerophospholipids ($n = 6$) and hydroxy acids ($n = 1$). In dataset B, the levels of 37 metabolites (9 annotated), were significantly different in MC compared with NC ($P < 0.05$) (Table 2, Table S1). The annotated

metabolites belong to the metabolite classes of amino acids ($n = 2$), purine nucleosides ($n = 1$), carboxylic acids ($n = 2$), fatty acyls ($n = 2$), and bile acids ($n = 2$). Of the annotated metabolites, threonine showed a significant difference between MC and NC in both datasets ($P < 0.05$). Six unannotated metabolites showed significant differences between MC and NC in both datasets (Table S1). 3-methylglutarylcarnitine, pyroglutamic acid, and glutamine showed a significant difference in one dataset and a tendency to a difference in the other ($P < 0.1$). Additionally, five unannotated metabolites showed a significant difference between MC and NC in one dataset and a tendency to a difference in the other (Table S1).

In addition, the correlation between all the metabolites that showed a significant difference between NC and MC in the two datasets, and the number of years that the samples have been in storage was tested. Years in storage was calculated as the difference between sampling date and analysis date. This was done to investigate if the observed differences could be due to the above described storage effect (Table S2). In dataset A, one unannotated metabolite had a significant correlation with years in storage. This metabolite was excluded from the cluster analysis and the pathway analysis. In dataset B, no metabolites had a significant association with years in storage. Similar correlation analyses were done between metabolite levels and participant age at the time of sampling, as well as the presence of at least one allele of *APOEε4* (Table S2). In dataset A, pyroglutamic acid and 2-oleoyl-GPC had a significant correlation with age at sampling ($P = 0.027$ and $P = 0.043$ respectively). In dataset B, no significant correlation was observed between any of the annotated metabolites and age at sampling. No significant correlation of metabolites with the presence of *APOEε4* was observed in either set.

Heatmaps (Fig. 1A and B) for the two datasets were generated based on the hierarchal clustering of both the

Table 2. Differentially expressed metabolites between presymptomatic MC and NC

Dataset	Metabolite	Metabolite class	Fold change	*P* value	Correlation to Aβ(1–42/1–40)
B	Glycohyocholic acid	Bile acids	−1.023	0.014	−0.236
B	Asymmetric dimethylarginine	Carboxylic acids	0.403	0.025	0.418
B	Ursodeoxycholic acid	Bile acids	2.193	0.025	−0.006
B	Threonine[1]	Amino acids	0.392	0.043	0.042
B	Asparagine	Amino acids	0.417	0.043	0.164
B	N2,N2-Dimethylguanosine	Purine nucleosides	0.649	0.043	0.139
B	N-Acetylvaline	Carboxylic acids	0.341	0.043	−0.018
B	3-Methylglutarylcarnitine[2]	Fatty acyls	−0.793	0.043	−0.382
B	2-Hydroxycaproic acid	Fatty Acyls	0.339	0.043	0.394
A	1-oleoyl-GPC	Glycerophospholipids	0.170	0.003	0.544
A	Cystine	Amino acids	−0.289	0.017	−0.341
A	Glutamine[2]	Amino acids	0.157	0.017	0.505
A	2-oleoyl-GPC	Glycerophospholipids	0.335	0.017	0.505
A	Pyroglutamic acid[2]	Carboxylic acids	0.153	0.024	0.544
A	Uric acid	Imidazopyrimidines	−0.496	0.024	−0.609*
A	1-Palmitoyl-sn-glycero-3-phosphocholine	Glycerophospholipids	0.436	0.024	0.390
A	1-arachidonoyl-GPC	Glycerophospholipids	0.337	0.024	0.401
A	3-Hydroxybutyric acid	Hydroxy acids	−0.731	0.024	−0.341
A	Glucose	Hexoses	−0.164	0.033	−0.571*
A	Threonine[1]	Amino acids	0.138	0.045	0.445
A	Propionylcarnitine	Fatty Acyls	−0.497	0.045	−0.374
A	2-stearoyl-GPC	Glycerophospholipids	0.264	0.045	0.220
A	1-docosapentaenoyl-GPC	Glycerophospholipids	0.342	0.045	0.648*

Annotated metabolites (n = 23) showed a significant (P < 0.05) difference between MC and NC. Log2 foldchange is shown as the difference between MC and NC, with positive values indicating higher relative metabolite levels in MC, and vice versa.
[1]Indicates the metabolite is significantly different between MC and NC in both dataset A and dataset B.
[2]Indicates that the metabolite is significantly different between MC and NC in one dataset and trending in the other (0.05 < P < 0.1).
*Significant correlation (P < 0.05) between metabolite and A$\beta_{1–42/1–40}$-ratio.

samples and the metabolites (Table 2, Table S1). In both datasets, the MC and the NC separate into two different clusters. Furthermore, the metabolites form two distinct clusters in both datasets as well, where one cluster of metabolites was found at higher levels in MC than in NC and the other shows the opposite trend (Fig. 1A and B).

Correlations between plasma metabolites and plasma A$\beta_{1–42}$/A$\beta_{1–40}$ ratio

Amyloid pathology is a hallmark of AD and Aβ levels in plasma are used as possible surrogate biomarkers.[24,25] It has been shown that *PSEN1*-H163Y exhibit higher levels of A$\beta_{1–42}$/A$\beta_{1–40}$ in in vitro assays.[4] We, therefore, tested the correlation between all 1199 metabolites and the ratio of A$\beta_{1–42}$/A$\beta_{1–40}$ in plasma (Table 3, Table S3). In dataset A, significant correlations were observed between 50 metabolites (12 annotated) and the ratio of A$\beta_{1–42}$/A$\beta_{1–40}$ (Table 3). In dataset B, significant correlations were observed between 55 metabolites (18 annotated) and the ratio of A$\beta_{1–42}$/A$\beta_{1–40}$. This includes glucose and uric acid, showing a negative correlation, and 1-docosapentaenoyl-GPC, showing positive correlations, which exhibit differential levels in MC

compared to NC (Table 3). None of the metabolites showed a significant correlation with the ratio of A$\beta_{1–42}$/A$\beta_{1–40}$ in both datasets. The distributions of the A$\beta_{1–42}$/A$\beta_{1–40}$ ratios in the two datasets are shown in Figure S3.

Biological significance of annotated metabolites

To examine the biological significance of 23 annotated metabolites from dataset A and dataset B, we performed the Ingenuity Pathway Analysis (IPA). Canonical pathways identified include "Asparagine Biosynthesis I," "tRNA Charging," "Asparagine Degradation I," "Glutamine Degradation I," and "IL-12 signaling and production in Macrophages" (Fig. 2A). Along with pathway enrichment, the IPA also enriched metabolites for two different categories "Disease and Disorders" and "Molecular and Cellular Functions" (Fig. S2). We explored these categories to understand the role of these metabolites in the presymptomatic MC. In "Molecular and Cellular functions," the metabolites were part of the cellular process "Lipid metabolism," "Cellular Growth and proliferation" (Fig. S2), "Peroxidation of lipid," "Production of reactive oxygen
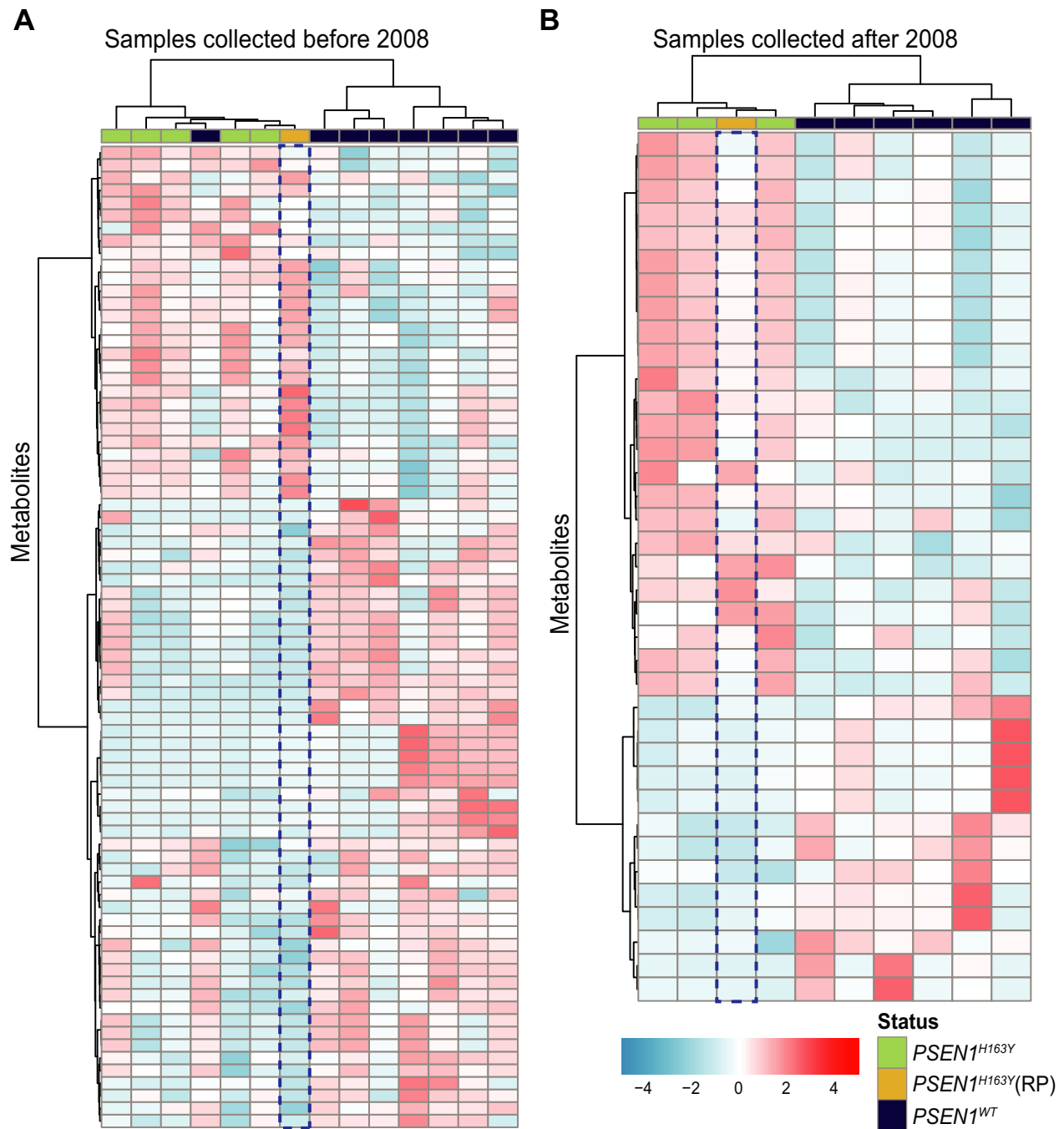
Figure 1. Heat map showing similarities between samples of the metabolites that were differentially expressed between NC (noncarrier group, dark blue) and the *PSEN1*-H163Y MC (mutation carrier group, Green). Sample from the reduced penetrance mutation carrier (RP) case is represented by yellow color. Legend: Red (upregulated metabolite), Blue (downregulated metabolite) and white (no modulation). (A) Samples from dataset A. (B) Samples from dataset B.

species," and "Neuronal cell death." In addition, under the category "Disease and Disorders" the metabolites were linked to the disease-related phenotypes including "Metabolic disease," "Endocrine system disorder," and "Chronic inflammatory disorder" (Fig. 2E and F, Fig. S2).

Metabolites are the functional endpoint of biological processes, which do not act alone and are regulated by upstream regulators at a given physiological condition.[26,27] Therefore, with the help of the "Upstream Regulator Analysis"[21] algorithm part of IPA, (supported by the

Table 3. Correlation between metabolites and plasma $A\beta_{1-42/1-40}$ ratio

Dataset	Metabolite	Metabolite class	Correlation to Aβ (1–42/1–40)	*P* value
B	2-methylguanosine	Purine Nucleosides	0.794	0.006
B	2-stearoyl-GPC	Glycerophospholipids	−0.794	0.006
B	Hypoxanthine	Imidazopyrimidines	−0.782	0.008
B	scyllo-Inositol	Organooxygens	−0.782	0.008
B	myo-Inositol	Organooxygens	−0.758	0.011
B	1-stearoyl-GPC	Glycerophospholipids	−0.758	0.011
B	2-methylglutaric acid	Fatty acyls	−0.758	0.011
B	Phenylalanylalanine	Carboxylic acids	−0.721	0.019
B	Valerylcarnitine	Fatty acyls	−0.721	0.019
B	Creatinine	Carboxylic acids	0.709	0.022
B	Indoleacetate	Indoles	−0.709	0.022
B	Tetradecanedioate	Fatty acyls	−0.709	0.022
B	Caffeic acid	Hydroxycinnamic acids	−0.697	0.025
B	Phenylalanylvaline	Carboxylic acids	−0.697	0.025
B	Pyroglutamic acid	Carboxylic acids	0.697	0.025
B	2 − Hydroxypalmitate	Fatty acyls	−0.673	0.033
B	Butyrylcarnitine	Fatty acyls	−0.661	0.038
B	Uracil	Diazines	0.661	0.038
A	Pipecolate	Carboxylic acids	−0.736	0.004
A	Phenylacetylglutamine	Carboxylic acids	−0.665	0.013
A	1-docosapentaenoyl-GPC	Glycerophospholipids	0.648	0.017
A	Serotonin	Indoles	−0.610	0.027
A	Uric acid	Imidazopyrimidines	−0.610	0.027
A	Octenoylcarnitine	Fatty acyls	−0.588	0.035
A	Cholic acid	Steroids	0.577	0.039
A	Glucose	Hexoses	−0.571	0.041
A	Hexadecanedioate	Fatty acyls	−0.566	0.044
A	Eicoseneoyl carnitine	Fatty acyls	−0.555	0.049
A	Inosine	Purine Nucleosides	−0.555	0.049
A	Malic acid	Hydroxy acids	−0.555	0.049

Spearman correlation between 1199 detected metabolites, in both dataset A and B, and $A\beta_{1-42/1-40}$ ratio. The table shows the annotated metabolites that show a significant correlation ($P < 0.05$).

Ingenuity® Knowledge Base) various, statistically significant, regulators of the 23 metabolites were identified (Table S4). These upstream regulators include the transcription factors TFE3 (Transcription factor E3), ZBTB20 (Zinc finger- and BTB domain-containing protein 20) and CEBPB (CCAAT-Enhancer Binding Protein-β). Moreover, along with transcription factors, IPA identified the enzymes DDAH2 (dimethylarginine dimethylaminohydrolase-2), RGS16 (Regulator of G Protein Signaling 16), FMO3 (flavin monooxygenase-3), and PIK3CA (phosphatidylinositol-4,5-bisphosphate 3-kinase alpha), which are part of regulatory networks. Furthermore, metabolites that are part of "Lipid metabolism" and "Cell cycle" were visualized using IPA (Fig. 3A and B).

Discussion

In this study, we performed an untargeted screening of plasma metabolites in male presymptomatic *PSEN1*-

H163Y MC known to exhibit brain glucose hypometabolism early in the preclinical phase, up to 20 years prior to expected onset age.[14] It has been reported that the plasma metabolome significantly varies between males and females.[28] Due to the nonavailability of female presymptomatic carriers, our study does not include plasma from female subjects. The presymptomatic metabolite profile identified in our study is therefore not confounded by any gender bias in the blood metabolite profile. *APOEε4* is represented in both MC and NC and metabolite correlation analysis did not indicate skewness.[28] In presymptomatic MC, amino acids, fatty acyls, carboxylic acids, hexoses, purine nucleosides, glycerophosphatidylcholines, and bile acids were significantly altered when compared to NC (Table 2). Interestingly, these classes of metabolites are also associated with sporadic AD.[1,5–7,9,10,29–32] Notably, we found asparagine, propionyl-l-carnitine, glycerophosphatidylcholine species, and asymmetric dimethylarginine (Table 2), which were part of the
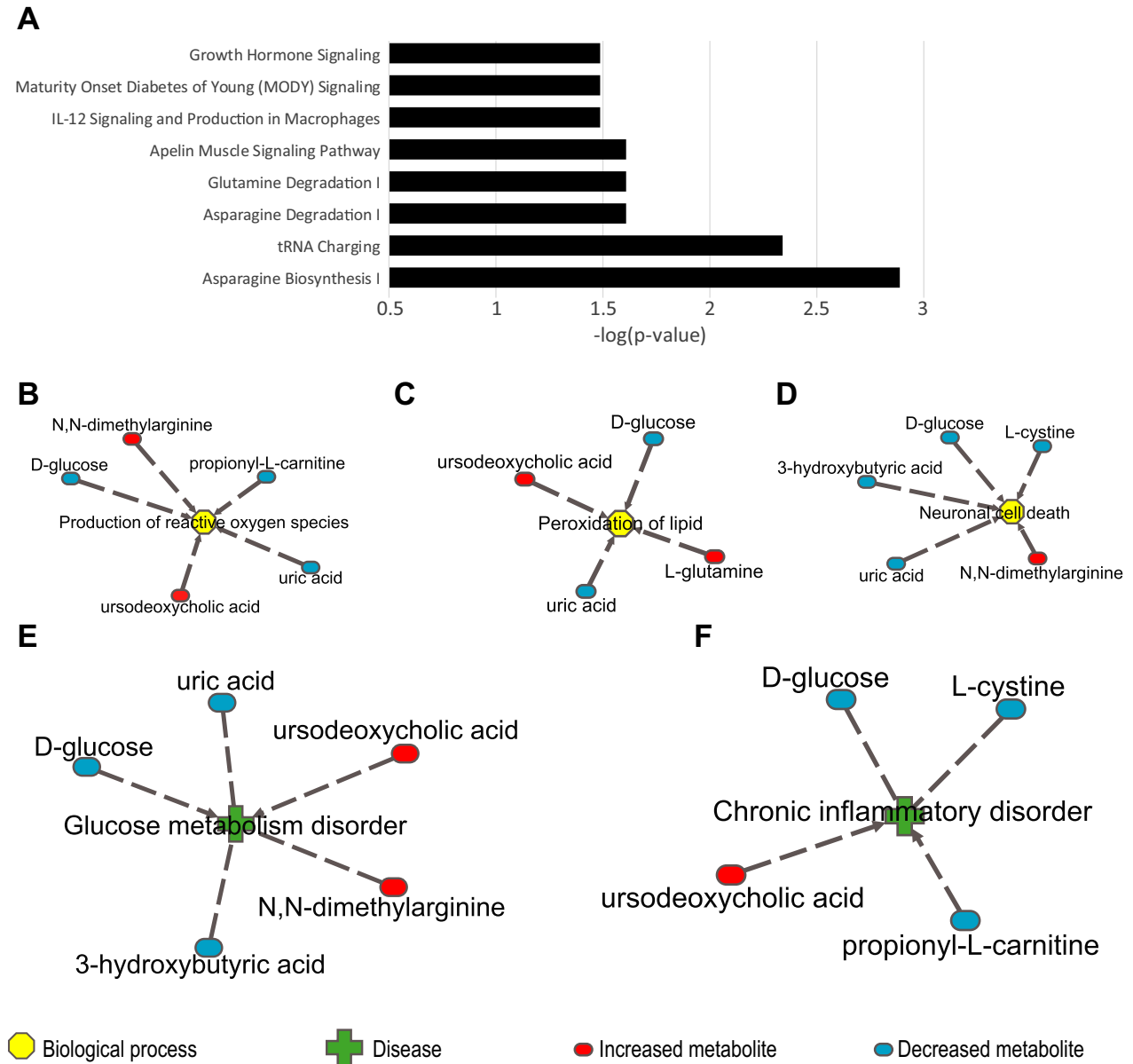
A

B   **C**   **D**

E   **F**

🟡 Biological process   ✚ Disease   🔴 Increased metabolite   🔵 Decreased metabolite

Figure 2. (A) Enriched canonical pathways for 23 annotated metabolites, which were differentially expressed between presymptomatic *PSEN1* MC and NC. (B–D) In "Molecular and Cellular Functions" terms, identified metabolites were associated with (B) "Production of reactive oxygen species" (C) "Peroxidation of lipid," (D) "Neuronal cell death". (E–F). In "Disease and Disorders" terms, under "Metabolic disease" (E) "Glucose metabolism disorder" and in "Inflammatory disease" (F) "Chronic inflammatory disorder" metabolite network was identified.

metabolite panel that previously has been reported to predict the clinical transition from presymptomatic to prodromal or symptomatic late-onset AD.[7]

We identified differential metabolites associated with "Production of reactive oxygen species," "lipid peroxidation," "glucose metabolism disorder," and "chronic inflammatory disorder" (Fig. 2, Fig. S2) which are known to be inherent of FAD pathobiology.[13,33–36] Amyloid-beta mediated mitochondrial dysfunction associated with

glucose hypometabolism is an indicator of molecular events, which precede amyloid aggregation.[37–39] Oligomeric forms of Aβ can give rise to oxidative stress placing themselves in the lipid bilayer which causes lipid peroxidation, at the end leading to neuronal cell death.[13,40,41] Furthermore, increased levels of 1-docosapentaenoyl-GPC (positive correlation), decreased levels of glucose (negative correlation), and uric acid (negative correlation) in MC were significantly correlated with A$\beta_{1–42}$/A$\beta_{1–40}$ (Table 2).
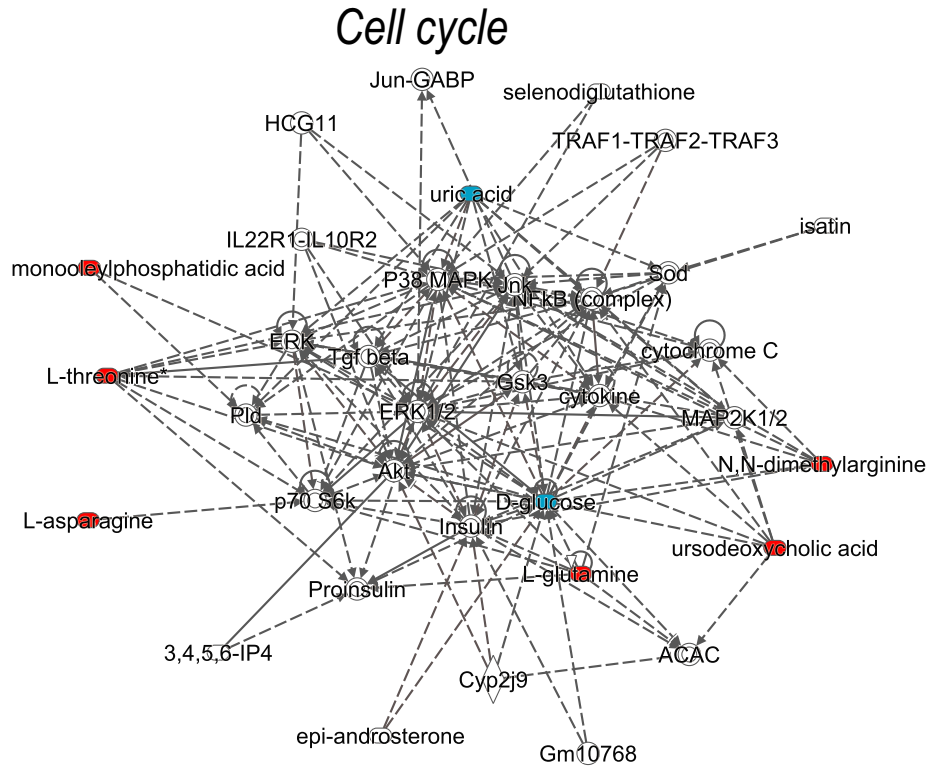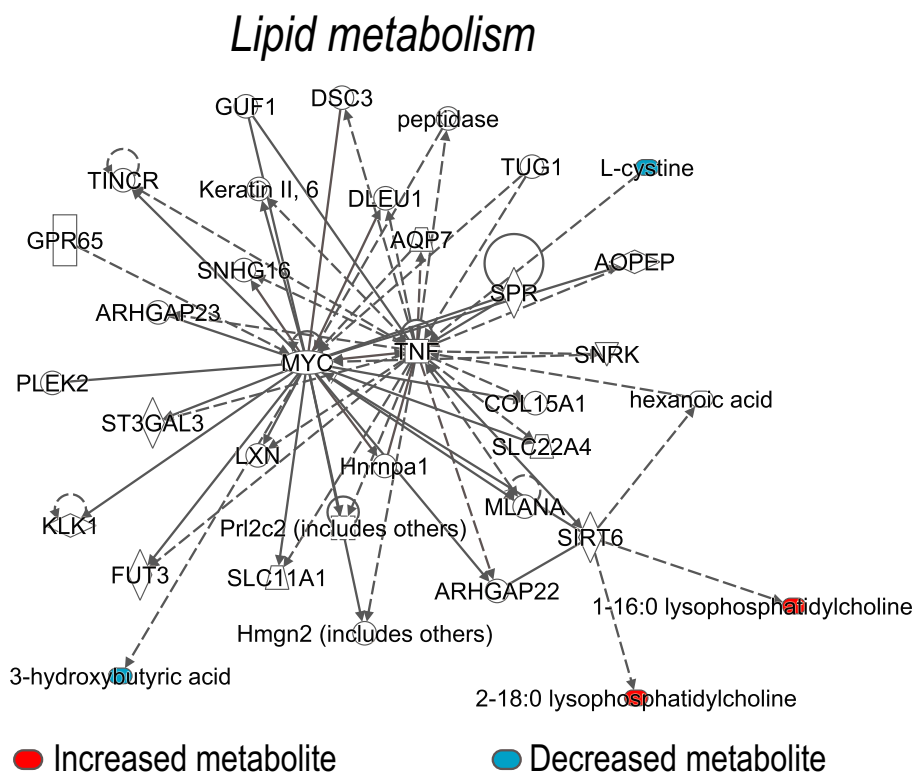
Figure 3. (A) Network of metabolites and its regulators involved in the "Cell cycle." (B) Molecular network of differentially expressed metabolites and their upstream regulators involved in the "Lipid metabolism."

Besides, several metabolites were significantly correlated with $A\beta_{1-42}/A\beta_{1-40}$, but not identified in the univariate analysis, probably due to a lack of statistical power (Table S3). Plasma $A\beta$ measurement is a growing frontier[25,42] and its measurement is associated with several challenges both technical and biological.[43,44] $A\beta$ measurement is affected by age,[45] gender,[46] body mass index,[47] and high density lipoproteins levels[47] of the subjects. Moreover, plasma $A\beta$ levels are associated with time to freezing blood samples as well as the volume of blood collected from the study subjects.[43,44] More recent studies have also indicated only weak correlations between plasma $A\beta$ levels and $A\beta$ levels measured in CSF and brain by PET-imaging, indicating limitations in the diagnostic value of plasma $A\beta$ with the current methodologies.[24] Furthermore, despite the difficulties of $A\beta$ measurements in plasma the variability due to between individual differences in $A\beta$ production or degradation is very much reduced when the ratio $A\beta_{1-42}/A\beta_{1-40}$ is used (as here), since it normalizes for this, and for possible variability due to preanalytical procedures (either sample handling and storage).[20] In mass spectrometry assays, isotope-labeled calibrators are also added to the samples before processing and analyses, which give more exact measures of the $A\beta_{1-42}/A\beta_{1-40}$ ratio as compared with then analyses are performed by separate immunoassays.[19,20] The suggested upstream regulators of the identified metabolites in our study are proposed to play a role in modulating different cellular events. In the event of mitochondrial dysfunction, TFE3 is activated and plays a vital role in regulating energy metabolism.[48] In addition, ZBTB20 is another upstream regulator that plays an essential role in glucose homeostasis.[49] Thus our results give several indications of a dysfunctional energy metabolism in AD.[11,26,33,37,50,51]

In the context of inflammation, astrocytes and microglia are the principal players in AD[26,52] and their activation is characteristic of the preclinical phase.[53] $A\beta$ activates microglia (Brain resident macrophages[54] which trigger a proinflammatory cascade, likely IL-12, and IL-23.[55–57] The metabolites found in our study (Fig. 2A) are associated with the IL-12 pathway. Activated microglia induce neurotoxic reactive astrocytes.[58] Moreover, the metabolite upstream-regulator CEBPB identified here, is activated by $A\beta$ in glial cells, which in turn initiates the inflammatory cascade.[59]

A rare case of *PSEN1*-H163Y reduced penetrance (RP)[15] is also part of our study. We included the plasma samples collected before the average age of onset in the family (52 ± 6) and the RP case exhibits a similar metabolic profile to the other MC (Fig. 1). Such reduced penetrance cases are rare and have been shown to have other protective genetic or environmental modifiers.[60] Further experimental studies employing single-cell genomics[61] and directly induced neurons from fibroblasts[62] can shed more light on possible mechanisms leading to resilience.

This pilot-scale study has its limitations. The study design is observational, it is difficult to control all the confounding factors, for example, the metabolite profile is highly influenced by lifetime immunological experience,[63] gut microbiota[64] and exposome.[65] Also, the medication history as well as preceding diet of the subjects and time of plasma sampling was not accounted for. However, a study evaluating fasting versus nonfasting, in the same individuals (i.e. repeat samples fasting and postprandial, incl. repeat samples), found no effects[66] on $A\beta_{1-42}$ or $A\beta1-40$. The metabolites found in dataset A and dataset B are not comparable rather they complement each other. Considering the low frequency of the *PSEN1* mutation carriers in our Swedish cohorts the sample size was small, and the *P* values were not corrected for multiple comparisons[11] in the univariate analysis. It has been shown that blood metabolites are strongly associated with age, yet their association is highly selective. In our analysis, we found pyroglutamic acid and 2-oleoyl-GPC to be correlated with age (Table S2).

Here, we report plasma metabolites and their upstream regulators and pathways, which were dysregulated in presymptomatic *PSEN1*-H163Y mutation carriers. These are consistent with previous findings of FAD pathophysiology. It is estimated that there are 25 424 blood metabolites[67,68] and due to contemporary technical limitations, a large fraction of them remain unannotated. In this study, we found several unannotated metabolites (Tables S1 and S3) that will be of significant interest to future FAD metabolomics studies. Understanding these unannotated metabolites will provide a comprehensive understanding of common metabolites that exist in both datasets A and B (Tables S1 and S3). However, results from this pilot study need to be evaluated in a larger FAD cohort. Considering the low frequency of FAD cases in the Swedish population, acquiring the optimal sample size for similar studies remains the biggest hurdle. The FAD cases can be highly informative on the cellular and molecular front when metabolomics are integrated with multi-omics datasets.[27,69]

Acknowledgments

Conflict of Interest

None.

Funding Information

Data Availability Statement

Datasets can be accessed at MetaboLights (https://www.eb i.ac.uk/metabolights/) with identifier MTBLS1721.

References

1. Toledo JB, Arnold M, Kastenmuller G, et al. Metabolic network failures in Alzheimer's disease: a biochemical road map. Alzheimers Dement 2017;13:965–984.

2. Thordardottir S, Kinhult Stahlbom A, Almkvist O, et al. The effects of different familial Alzheimer's disease mutations on APP processing in vivo. Alzheimers Res Ther 2017;9:9.

3. Van Cauwenberghe C, Van Broeckhoven C, Sleegers K. The genetic landscape of Alzheimer disease: clinical implications and perspectives. Genet Med 2016;18:421–430.

4. Sun L, Zhou R, Yang G, Shi Y. Analysis of 138 pathogenic mutations in presenilin-1 on the in vitro production of Abeta42 and Abeta40 peptides by gamma-secretase. Proc Natl Acad Sci USA 2017;114:E476–E485.

5. Jiang Y, Zhu Z, Shi J, et al. Metabolomics in the development and progression of dementia: a systematic review. Front Neurosci 2019;13:343.

6. Mapstone M, Lin F, Nalls MA, et al. What success can teach us about failure: the plasma metabolome of older adults with superior memory and lessons for Alzheimer's disease. Neurobiol Aging 2017;51:148–155.

7. Fiandaca MS, Zhong X, Cheema AK, et al. Plasma 24-metabolite panel predicts preclinical transition to clinical stages of Alzheimer's disease. Front Neurol 2015;6:237.

8. Trushina E, Dutta T, Persson X-MT, et al. Identification of altered metabolic pathways in plasma and CSF in mild cognitive impairment and Alzheimer's disease using metabolomics. PLoS One 2013;8:e63644.

9. Lin CN, Huang CC, Huang KL, et al. A metabolomic approach to identifying biomarkers in blood of Alzheimer's disease. Ann Clin Transl Neurol 2019;6:537–545.

10. Wilkins JM, Trushina E. Application of metabolomics in Alzheimer's disease. Front Neurol 2018;8:719.

11. Chatterjee P, Lim WL, Shui G, et al. Plasma phospholipid and sphingolipid alterations in presenilin1 mutation carriers: a pilot study. J Alzheimers Dis 2016;50:887–894.

12. Kaiser NC, Melrose RJ, Liu C, et al. Neuropsychological and neuroimaging markers in early versus late-onset Alzheimer's disease. Am J Alzheimer's Dis Other Dement 2012;27:520–529.

13. Mosconi L, Pupi A, De Leon MJ. Brain glucose hypometabolism and oxidative stress in preclinical Alzheimer's disease. Ann N Y Acad Sci 2008;1147:180–195.

14. Scholl M, Almkvist O, Axelman K, et al. Glucose metabolism and PIB binding in carriers of a His163Tyr presenilin 1 mutation. Neurobiol Aging 2011;32:1388–1399.

15. Thordardottir S, Rodriguez-Vieitez E, Almkvist O, et al. Reduced penetrance of the PSEN1 H163Y autosomal dominant Alzheimer mutation: a 22-year follow-up study. Alzheimers Res Ther 2018;10:45.

16. Axelman K, Basun H, Lannfelt L. Wide range of disease onset in a family with Alzheimer disease and a His163Tyr mutation in the presenilin-1 gene. Arch Neurol 1998;55:698–702.

17. Almkvist O, Rodriguez-Vieitez E, Thordardottir S, et al. Predicting cognitive decline across four decades in mutation carriers and non-carriers in autosomal-dominant Alzheimer's disease. J Int Neuropsychol Soc 2017;23:195–203.

18. Diamanti K, Cavalli M, Pan G, et al. Intra- and inter-individual metabolic profiling s carnitine and lysophosphatidylcholine pathways as key molecular defects in type 2 diabetes. Sci Rep 2019;9:9653.

19. Pannee J, Tornqvist U, Westerlund A, et al. The amyloid-beta degradation pattern in plasma–a possible tool for clinical trials in Alzheimer's disease. Neurosci Lett 2014;573:7–12.

20. Pannee J, Portelius E, Oppermann M, et al. A selected reaction monitoring (SRM)-based method for absolute quantification of Abeta38, Abeta40, and Abeta42 in cerebrospinal fluid of Alzheimer's disease patients and healthy controls. J Alzheimers Dis 2013;33:1021–1032.

21. Kramer A, Green J, Pollard J Jr, Tugendreich S. Causal analysis approaches in Ingenuity Pathway Analysis. Bioinformatics 2014;30:523–530.

22. Folstein MF, Folstein SE, McHugh PR. "Mini-mental state". A practical method for grading the cognitive state of patients for the clinician. J Psychiatr Res 1975;12:189–198.

23. Wagner-Golbs A, Neuber S, Kamlage B, et al. Effects of long-term storage at -80 degrees C on the human plasma metabolome. Metabolites 2019;9:99.

24. Janelidze S, Stomrud E, Palmqvist S, et al. Plasma beta-amyloid in Alzheimer's disease and vascular disease. Sci Rep 2016;6:26801.

25. Hampel H, O'Bryant SE, Molinuevo JL, et al. Blood-based biomarkers for Alzheimer disease: mapping the road to the clinic. Nat Rev Neurol 2018;14:639–652.

26. Johnson ECB, Dammer EB, Duong DM, et al. Large-scale proteomic analysis of Alzheimer's disease brain and cerebrospinal fluid reveals early changes in energy metabolism associated with microglia and astrocyte activation. Nat Med 2020;26:769–780.

27. Pinu FR, Beale DJ, Paten AM, et al. Systems biology and multi-omics integration: viewpoints from the metabolomics research community. Metabolites. 2019;9:76.

28. Arnold M, Nho K, Kueider-Paisley A, et al. Sex and APOE epsilon4 genotype modify the Alzheimer's disease serum metabolome. Nat Commun 2020;11:1148.

29. Nho K, Kueider-Paisley A, MahmoudianDehkordi S, et al. Altered bile acid profile in mild cognitive impairment and Alzheimer's disease: relationship to neuroimaging and CSF biomarkers. Alzheimers Dement 2019;15:232–244.

30. MahmoudianDehkordi S, Arnold M, Nho K, et al. Altered bile acid profile associates with cognitive impairment in Alzheimer's disease-an emerging role for gut microbiome. Alzheimers Dement 2019;15:76–92.

31. Varma VR, Oommen AM, Varma S, et al. Brain and blood metabolite signatures of pathology and progression in Alzheimer disease: a targeted metabolomics study. PLoS Med 2018;15:e1002482.

32. Olazaran J, Gil-de-Gomez L, Rodriguez-Martin A, et al. A blood-based, 7-metabolite signature for the early diagnosis of Alzheimer's disease. J Alzheimers Dis 2015;45:1157–1173.

33. Kuehn BM. In Alzheimer research, glucose metabolism moves to center stage. JAMA 2020;323:297.

34. Heneka MT, Carson MJ, El Khoury J, et al. Neuroinflammation in Alzheimer's disease. Lancet Neurol 2015;14:388–405.

35. Hauptmann S, Scherping I, Drose S, et al. Mitochondrial dysfunction: an early event in Alzheimer pathology accumulates with age in AD transgenic mice. Neurobiol Aging 2009;30:1574–1586.

36. Mosconi L, Sorbi S, de Leon MJ, et al. Hypometabolism exceeds atrophy in presymptomatic early-onset familial Alzheimer's disease. J Nucl Med 2006;47:1778–1786.

37. Teo E, Ravi S, Barardo D, et al. Metabolic stress is a primary pathogenic event in transgenic Caenorhabditis elegans expressing pan-neuronal human amyloid beta. Elife 2019;8:e50069.

38. Ciavardelli D, Piras F, Consalvo A, et al. Medium-chain plasma acylcarnitines, ketone levels, cognition, and gray matter volumes in healthy elderly, mildly cognitively impaired, or Alzheimer's disease subjects. Neurobiol Aging 2016;43:1–12.

39. Yao J, Irwin RW, Zhao L, et al. Mitochondrial bioenergetic deficit precedes Alzheimer's pathology in female mouse model of Alzheimer's disease. Proc Natl Acad Sci USA 2009;106:14670–14675.

40. Pena-Bautista C, Vigor C, Galano JM, et al. New screening approach for Alzheimer's disease risk assessment from urine lipid peroxidation compounds. Sci Rep 2019;9:14244.

41. Tonnies E, Trushina E. Oxidative stress, synaptic dysfunction, and Alzheimer's disease. J Alzheimers Dis 2017;57:1105–1121.

42. O'Bryant SE, Mielke MM, Rissman RA, et al. Blood-based biomarkers in Alzheimer disease: current state of the science and a novel collaborative paradigm for advancing from discovery to clinic. Alzheimers Dement 2017;13:45–58.

43. Figurski MJ, Waligórska T, Toledo J, et al. Improved protocol for measurement of plasma β-amyloid in longitudinal evaluation of Alzheimer's Disease Neuroimaging Initiative study patients. Alzheimers Dement 2012;8:250–260.

44. Toledo JB, Shaw LM, Trojanowski JQ. Plasma amyloid beta measurements - a desired but elusive Alzheimer's disease biomarker. Alzheimers Res Ther 2013;5:8.

45. Huang Y, Potter R, Sigurdson W, et al. β-amyloid dynamics in human plasma. Arch Neurol 2012;69:1591–1597.

46. Metti AL, Cauley JA, Ayonayon HN, et al. The demographic and medical correlates of plasma aβ40 and aβ42. Alzheimer Dis Assoc Disord 2013;27:244–249.

47. Mayeux R, Honig LS, Tang M-X, et al. Plasma Aβ40 and Aβ42 and Alzheimer's disease. Relation Age Mortality Risk 2003;61:1185–1190.

48. Raben N, Puertollano R. TFEB and TFE3: linking lysosomes to cellular adaptation to stress. Annu Rev Cell Dev Biol 2016;32:255–278.

49. Sutherland AP, Zhang H, Zhang Y, et al. Zinc finger protein Zbtb20 is essential for postnatal survival and glucose homeostasis. Mol Cell Biol 2009;29:2804–2815.

50. Sato N, Morishita R. The roles of lipid and glucose metabolism in modulation of beta-amyloid, tau, and neurodegeneration in the pathogenesis of Alzheimer disease. Front Aging Neurosci 2015;7:199.

51. Zhu TB, Zhang Z, Luo P, et al. Lipid metabolism in Alzheimer's disease. Brain Res Bull 2019;144:68–74.

52. Kinney JW, Bemiller SM, Murtishaw AS, et al. Inflammation as a central mechanism in Alzheimer's disease. Alzheimer's Dement 2018;4:575–590.

53. Long JM, Holtzman DM. Alzheimer disease: an update on pathobiology and treatment strategies. Cell 2019;179:312–339.

54. Bennett ML, Bennett FC. The influence of environment and origin on brain resident macrophages and implications for therapy. Nat Neurosci 2020;23:157–166.

55. Kreisl WC. Discerning the relationship between microglial activation and Alzheimer's disease. Brain 2017;140:1825–1828.

56. Vom Berg J, Prokop S, Miller KR, et al. Inhibition of IL-12/IL-23 signaling reduces Alzheimer's disease-like pathology and cognitive decline. Nat Med 2012;18:1812–1819.

57. Hansen DV, Hanson JE, Sheng M. Microglia in Alzheimer's disease. J Cell Biol 2018;217:459–472.

58. Liddelow SA, Guttenplan KA, Clarke LE, et al. Neurotoxic reactive astrocytes are induced by activated microglia. Nature 2017;541:481–487.

59. Wang ZH, Gong K, Liu X, et al. C/EBPbeta regulates delta-secretase expression and mediates pathogenesis in mouse models of Alzheimer's disease. Nat Commun 2018;9:1784.

60. Arboleda-Velasquez JF, Lopera F, O'Hare M, et al. Resistance to autosomal dominant Alzheimer's disease in an APOE3 Christchurch homozygote: a case report. Nat Med 2019;25:1680–1683.

61. Mathys H, Davila-Velderrain J, Peng Z, et al. Single-cell transcriptomic analysis of Alzheimer's disease. Nature 2019;570:332–337.

62. Drouin-Ouellet J, Lau S, Brattås PL, et al. REST suppression mediates neural conversion of adult human fibroblasts via microRNA-dependent and -independent pathways. EMBO Mol Med. 2017;9:1117–1131.

63. Zmora N, Bashiardes S, Levy M, Elinav E. The role of the immune system in metabolic health and disease. Cell Metab 2017;25:506–521.

64. Mahmoudian Dehkordi S, Arnold M, Nho K, et al. Altered bile acid profile associates with cognitive impairment in Alzheimer's disease—an emerging role for gut microbiome. Alzheimer's Dement 2019;15:76–92.

65. Athersuch TJ, Keun HC. Metabolic profiling in human exposome studies. Mutagenesis 2015;30:755–762.

66. Bjerke M, Portelius E, Minthon L, et al. Confounding factors influencing amyloid Beta concentration in cerebrospinal fluid. Int J Alzheimer's Dis 2010;2010:1–11.

67. Darst BF, Koscik RL, Hogan KJ, et al. Longitudinal plasma metabolomics of aging and sex. Aging 2019;11:1262–1282.

68. Wishart DS, Feunang YD, Marcu A, et al. HMDB 4.0: the human metabolome database for 2018. Nucleic Acids Res 2018;46(D1):D608–D617.

69. Hasin Y, Seldin M, Lusis A. Multi-omics approaches to disease. Genome Biol 2017;18:83.

Supporting Information

Additional supporting information may be found online in the Supporting Information section at the end of the article.

Figure S1. PCA of all 24 plasma samples in the study, which were analyzed for 1199 metabolites in an untargeted manner.

Figure S2. List of GO terms under the category of "Molecular and Cellular Functions" and "Disease and Disorders," which were enriched for the 23 annotated metabolites in the Ingenuity Pathway Analysis (IPA).

Figure S3. Boxplot showing the distribution of the $A\beta_{1-42}/A\beta_{1-40}$ ratio for dataset A (left) and dataset B (right).

Table S1. The unannotated metabolites presented as "mass@retention time," that showed a significant ($P < 0.05$) difference between MC and NC. Log2 fold-change shown as the difference between MC and NC, with positive values indicating higher relative metabolite levels in MC, and vice versa.

Table S2. The Spearman's correlation between 23 metabolites and age at the time of sampling, number of storage years and presence of *APOEɛ4* allele ($P < 0.05$ value was considered as significant).

Table S3. Spearman correlation between 1199 detected metabolites, in both dataset "A" and "B", and $A\beta_{1-42/1-40}$-ratio.

Table S4. List of upstream regulators, which were enriched for the 23 annotated metabolites in the Ingenuity Pathway Analysis (IPA).

Data S1. Methodological description of plasma metabolite profiling using mass spectrometry.